



Development and characterization of hybrid films based on agar and alizarin red S for applications as non-enzymatic sensors for hydrogen peroxide

Maria de Fátima Cardoso Soares^{1,2}, Emanuel Airton de Oliveira Farias¹, Durcilene Alves da Silva^{1,3}, and Carla Eiras^{1,3,*}

¹Núcleo de Pesquisa em Biodiversidade e Biotecnologia, BIOTEC, Campus Ministro Reis Velloso, CMRV, Universidade Federal do Piauí, UFPI, Parnaíba, Brazil

²Instituto Federal de Educação, Ciência e Tecnologia do Piauí, IFPI, Campus Parnaíba, Parnaíba, PI 64210260, Brazil

³Laboratório Interdisciplinar de Materiais Avançados, LIMAV, CCN, UFPI, Teresina, PI 64049-550, Brazil

Received: 7 January 2016

Accepted: 5 April 2016

Published online:

2 May 2016

© Springer Science+Business
Media New York 2016

ABSTRACT

For the first time, the dye alizarin red S (ARS) was immobilized on indium tin oxide (ITO) electrodes via a layer-by-layer technique (LbL). This was achieved only when ARS was interspersed with the polymers agar (extracted from seaweed *Gracilaria birdiae*) and PAH [poly(allylamine hydrochloride)]. ARS alone did not show electroactivity when adsorbed onto ITO. Single-walled carbon nanotubes (functionalized with COOH, denoted CNTs) were used to increase the electrochemical signal of the LbL system. Interactions at the molecular level between the CNTs and other materials used in the construction of the films accounted for a threefold increase in the current signal of ARS. The films were developed as trilayer films of agar/PAH/ARS or agar(CNT)/PAH(CNT)/ARS and characterized by differential pulse voltammetry (DPV) and UV-visible spectroscopy and scanning electron microscopy. From the results, it was also possible to calculate the energy diagram for both films. The results showed that the films are promising for applications as electrochemical sensors. Accordingly, the agar(CNT)/PAH(CNT)/ARS film was tested for the reduction of hydrogen peroxide (H₂O₂). Under a constant potential of -0.5 V versus SCE (saturated calomel electrode), the film exhibited a rapid response for the reduction of peroxide (less than 5 s), and the current stabilized approximately at 30 s. The limit of detection for the amperometric sensor was approximately $0.15 \mu\text{mol L}^{-1}$.

Address correspondence to E-mail: carla.eiras.ufpi@gmail.com

Introduction

Nanotechnology is a multidisciplinary science that has produced countless applications in many sectors, such as industry, technology, and biotechnology, in addition to presenting high-economic value [1, 2]. The uniqueness of nanotechnology is not limited to the control and manipulation of individual molecules or the development of nanostructures; it also offers the possibility of developing new materials from the combination of chemical and physical characteristics of different materials, allowing new technological applications for these materials [3].

Among the areas of interest involving nanotechnology, the study of thin films has been explored for immobilizing various types of materials, enabling the manipulation of matter in an organized way at the atomic or molecular level [4]. Among the most common techniques used in the production of such films, include casting, spin coating [5], dip coating [6], Langmuir–Blodgett (LB) technique [7], and layer-by-layer (LbL) techniques [8]. However, LB and LbL techniques are the most used when the formation of highly organized thin films that favor the appearance of synergistic effects between different materials in the film.

The first implementation of layer-by-layer technique is attributed to Iler [9] using microparticles. The method was later revitalized by Decher [10], with the discovery of its applicability to a wide range of polyelectrolytes. The Decher proposal was mainly based on the electrostatic interactions between species of opposite charge; however, currently is known about other types of interactions that may occur, such as Van der Waals interactions, hydrogen bonding, or even biospecific interactions [11, 12]. More recently, the literature describes non-covalent interaction between two or more species, producing highly complex structures, which is known as constitutional dynamic chemistry (CDC) [13].

The LbL technique is also known for producing highly stable adsorbent layers. A wide variety of materials can be used in the LbL technique [14], such as proteins [15–17], enzymes [18–20], conductive polymers [21, 22], polysaccharides [23–25], and dyes, [26].

Dyes are examples of organic substances that have considerable versatility in terms of applications, ranging from dyeing of fabrics and food coloring to other fields of modern technology such as sunlight-

absorbing cells, as well as electronic and optical devices, including light emitting diodes (LED) as photosensitizers used for controlling microbial proliferation [27, 28].

Among the variety of available dyes, alizarin red S (ARS) stands out. ARS is a soluble derivative of alizarin (Alz) containing a non-reactive sulfonic group that is responsible for improving the solubility of the compound in aqueous media, Fig. 1 [29].

Initially, ARS was used as a colorimetric analytical reagent for spectrophotometric reactions [30]. However, some studies proposed the use of ARS as a surface modifier for solid electrodes for application as electrochemical sensors [31]. Most of these sensors have been produced using carbon electrodes [32–34], glassy carbon [35, 36], carbon nanotubes [37, 38], graphene [39], gold [40, 41], boron-doped diamond [42], or pyrolytic graphite [43, 44]. However, there are no reports in the literature on ARS adsorbed on ITO electrodes. This fact provides an opportunity for a characterization and study of the electrochemical, spectroscopic, and morphological properties of this compound.

Natural polysaccharides are another class of materials that have aroused interest for the production of LbL films [45–47]. Agar stands out among these polysaccharides because of its anticoagulant, antitumor, antiviral, and anti-inflammatory properties [48] that have resulted in applications in medicine, food, cosmetics, biotechnology, textiles, pharmaceuticals, and others [49–51]. The wide applicability of agar is linked to its ability to form gels (gelling, viscosifying, and/or emulsifying agents) and be non-toxic [52]. One of the nanotechnology's interests is to find new applications for these polysaccharides, such as their use in the production of films for use as an active layer for sensors and biosensors [53, 54].

Many types of sensors and biosensors have been developed for the detection of hydrogen peroxide (H_2O_2). Monitoring the levels of H_2O_2 is very important because it is a powerful oxidant and oxygenator

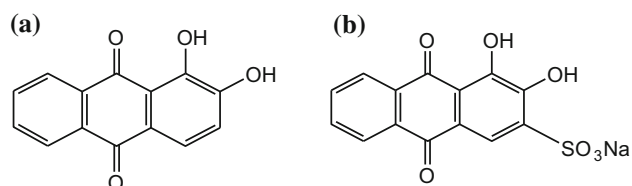


Figure 1 Structure of alizarin (Alz) and alizarin red S ARS.

that is essential for human immune response [55]. H_2O_2 is also important for the metabolism of proteins, carbohydrates, fats, vitamins, and minerals. In addition, H_2O_2 is involved in the regulation of blood sugar and in the energy production of body cells [52]. For these reasons, several studies aimed at the construction of sensors and biosensors for the detection of H_2O_2 have been conducted [54–57].

H_2O_2 also has an application in the textile industry and in the composition of cleaning products, such as detergent [54], as well as in the water purification industry [58]. Several analytical methods have been developed for the determination of H_2O_2 , such as chromatography, titration, chemiluminescence, spectrometry, and electrochemistry. Among these methods, electrochemical sensors have been shown to be an excellent alternative because of their speed of analysis, low cost, high sensitivity, and good selectivity. These attributes have motivated the production of various electrochemical sensors and biosensors for the detection/reduction of H_2O_2 [55, 59–62].

Most electrochemical sensors developed for H_2O_2 detection use enzymes to reduce the peroxide [63–68]. However, the use of enzymes for the development of electrochemical sensors has some drawbacks, including high cost and specific requirements under different environmental conditions.

In this study, for the first time, ARS was immobilized on ITO together with agar using LbL for the development of a non-enzymatic sensor able to detect H_2O_2 . The union of the anionic layers of these materials occurs through the use of PAH, a cationic polymer widely used for the production of self-assembled films. CNTs were also used to improve the electrochemical response of ARS.

The objective of this study is the development and characterization of LbL films based on agar, PAH, and ARS immobilized on ITO electrodes. These films were first characterized by differential pulse voltammetry (DPV) and UV–visible spectroscopy (UV–Vis). The films were then used for the reduction of hydrogen peroxide.

Experimental procedure

Materials

ARS was purchased from Merck. PAH and CNTs (functionalized with $-\text{COOH}$ groups) were purchased

from Sigma-Aldrich. ARS, PAH, and CNT were used as received. Agar was extracted from *Gracilaria birdiae* collected in the Piauı coastline and subsequently purified as described elsewhere [48].

Preparation of the solutions used for the adsorption of the films

The ARS and agar solutions were prepared at a concentration of 0.2 and 0.1 %, respectively. Ultra-pure water was employed as the solvent for both solutions. The PAH solution was prepared at 0.1 % using 0.1 % acetic acid as the solvent.

Durability test of sensor

A 0.1 mol L^{-1} of H_2O_2 solution was used for the tests for the reduction of hydrogen peroxide. In the durability test, the higher concentration of linear range was considered (8.0 mmol L^{-1}) and an applied potential of -0.6 V for 5 min. After this time, the electrode was washed in PBS 0.1 mol L^{-1} (pH 7.2) and the voltammogram of DPV was recorded in the supporting electrolyte in the absence of H_2O_2 . Then, the response of the film was compared before and after contact with peroxide.

LbL film adsorption

For the formation of LbL films, CNTs were dispersed separately in both agar and PAH solutions. Subsequently, a pre-cleaned ITO sample [69] was immersed in the agar(CNT) solution for 5 min. Then, the ITO/agar(CNT) system was dipped in pure water to remove the unadsorbed material, and then dried under N_2 flow. In the next step, the ITO/agar(CNT) electrode was dipped into the solution of PAH(CNT) for 5 min, washed, and then dried with N_2 , thereby forming a bilayer of ITO/agar(CNT)/PAH(CNT). Then, the ITO/agar(CNT)/PAH(CNT) system was immersed in the ARS solution for 5 min with washing and drying with N_2 as before. At the end of this process, a film containing the three-layer architecture ITO/agar(CNT)/PAH(CNT)/ARS was obtained.

For comparative studies, films were also prepared in the absence of CNTs, i.e., ITO/agar/PAH/ARS films, and films in the absence of an electroactive material, i.e., films of ITO/agar/PAH. We also tested the influence of the sequence of deposition of materials of interest versus the electrochemical response.

Characterization

The extracted polysaccharides were characterized by infrared spectroscopy on KBr pellets using a Shimadzu 8300 FTIR spectrometer. The analysis of zeta potential and molecular weight (MW) was performed by light scattering on a Malvern Zetasizer Nano ZS Model 3600 using a 633 nm laser at a fixed scattering angle of 173°. The sulfate content in carrageenan and agar was obtained by inductively coupled plasma optical emission spectrometry (ICP-OES) (Spectro, model across).

For the electrochemical characterization of the LbL films, a potentiostat/galvanostat Model 128 N AUTOLAB PGSTAT and an electrochemical cell with a 10.0-mL capacity with a lid for fitting three electrodes. A saturated calomel electrode (SCE) was used as the reference electrode and a platinum plate ($A = 2.0 \text{ cm}^2$) was used as the auxiliary electrode. The self-assembled film adsorbed on ITO ($A = 0.32 \text{ cm}^2$) was used as the working electrode. All analyses were performed using 0.1 M potassium phosphate buffer (pH 7.2) as the electrolyte at room temperature (22 °C).

The formation of multilayers was monitored by UV-visible spectroscopy (SHIMADZU Model UV-1800). The self-assembled films were adsorbed on common glass and a spectrum was measured after each 2 trilayers adsorbed, for a total of 20 trilayers and 10 spectra.

The morphological analysis of the films was conducted by SEM (equipment FEI, model Quanta FEG 250).

Results and discussion

Characterization of polysaccharide

The characterization of agar by FTIR was performed with the objective of identifying the sulfate groups

and 3,6-anhydrogalactose units that characterize the polysaccharide structure. Furthermore, these groups are responsible for the negative charges on the polysaccharide [70].

In Fig. 2, the spectrum presents some characteristic bands of polysaccharides, such as the C–O–C stretching vibration of glycosidic bonds, which are observed at 1158 and 1077 cm^{-1} . Moreover, the presence of the less intense band at 1250 cm^{-1} suggests the existence of a small percentage of sulfate groups in the polysaccharide structure, confirming its negative charge.

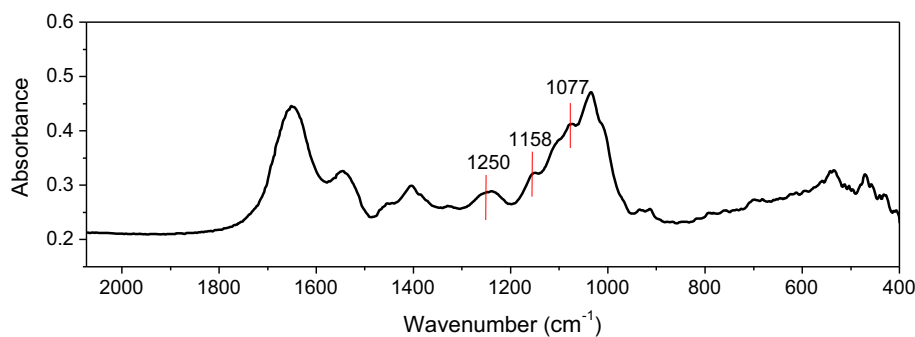
The agar molecular weight obtained by dynamic light scattering (DLS) was estimated at 1.4×10^3 kDa. The sulfate percentage present in the polysaccharide and the zeta potential of the solution used to prepare the films were estimated at 2.73 % and -30.4 mV, respectively.

Electrochemical characterization of LbL films

Figure 3 shows the voltammograms obtained by differential pulse voltammetry (DPV) for the films prepared with a bi- or trilayer structure in the presence and absence of CNTs. The response of an unmodified ITO electrode is also shown for comparison. An attempt was made to characterize these films by cyclic voltammetry (CV), though the redox processes had become more defined when obtained by differential pulse voltammetry (Fig. S1).

Under the experimental conditions employed, ITO did not show any redox response (see Fig. 3). When the ITO was modified with the agar/PAH bilayer film, no redox response was observed, as expected, since neither agar nor PAH are electroactive materials. For the case where CNTs were dispersed in agar and PAH solutions producing the agar(CNT)/PAH(CNT) bilayer film, a slight oxidation process at

Figure 2 Agar FTIR spectrum.



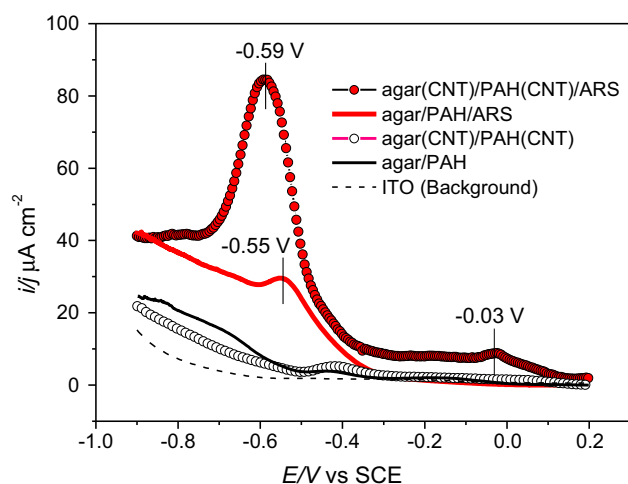


Figure 3 Differential pulse voltammograms obtained for bilayer and trilayer films containing or not containing CNTs dispersed in the solutions of interest. All measurements were carried out in 0.1 mol L^{-1} potassium phosphate (pH 7.2), $E_i = -0.9 \text{ V}$, $E_f = 0.2 \text{ V}$, $v = 25 \text{ mV s}^{-1}$.

-0.45 V versus SCE was observed, which can be attributed to the functionalized nanotubes present in the bilayer film.

Also in Fig. 3, the response of trilayer films where ARS was adsorbed on the outermost layer of the film is shown (agar/PAH/ARS film). We also compared the presence and absence of CNTs in this architecture. For the agar/PAH/ARS film, there was observed a well-defined oxidation process at -0.55 V versus SCE, which is assigned to the *p*-quinone group of ARS, as described in the literature [43–71].

Apparently, ARS has low adsorption or electroactivity when adsorbed on ITO, which justifies its use as a modifier of mainly carbon-based electrodes [32, 33]. When ARS was adsorbed on ITO, the response was similar to the clean electrode (data not shown). However, modification of the ITO electrode with the agar/PAH film allowed ARS adsorption in this system, but with a low current value ($29.5 \mu\text{A cm}^{-2}$ at -0.55 V). On the other hand, the introduction of CNTs into the structure of the film improved the electrochemical response of ARS, and the process defined before at -0.55 V shifted to -0.59 V with a current value of $84.5 \mu\text{A cm}^{-2}$, i.e., almost 3 times greater than that currently obtained for the agar/PAH/ARS film without CNTs (Fig. 3).

Several studies have reported interactions of ARS with the π electrons present in structures of carbon, such as glassy carbon [36, 37] and pyrolytic graphite

electrodes [19, 44] of the form that enhances the electrochemical signal of this compound. Such interactions can explain the increase of current caused by the presence of CNTs in the film.

In our studies, the appearance of a new oxidation process at -0.03 V for the agar(CNT)/PAH(CNT)/ARS film was also observed. This process only occurs when there is the presence of all materials interspersed in the film. This effect can be explained as an electrochemical process caused by a CDC interaction, which has been observed by other authors [13] in films containing single-walled carbon nanotubes dispersed in the polymeric matrix of chitosan and interspersed with cobalt phthalocyanine (Chit-SWCNTs/CoTsPc). Luz et al. [13] observed that the incorporation of SWCNTs also affected the morphology of the film, and caused an increase in the faradaic current, indicating a possible charge transfer interaction between cobalt phthalocyanine and SWCNTs.

Beyond agar, other polysaccharides, such as carrageenan (*Hypnea musciformis*) and cashew gum (*Anacardium occidentale*), were tested as a replacement for agar, as well as interspersed in hybrid films with the materials of interest. However, the best results were found using agar. The voltammograms for LbL films where carrageenan and gum of cashew were employed as agar replacements are shown in the supplementary material (Fig. S2).

Evidently, natural polysaccharides are excellent biomaterial alternatives for the development of thin films for different applications. The literature reports chitosan-based films for detecting heavy metals in contaminated waters [72, 73], cellulose-based films for detecting glucose [39] or chromium(VI) [74], and seaweed polysaccharides for Cr(VI) detection [75], and other films for the development of sensors based on many types of natural polysaccharides [76].

ARS was maintained as the outermost layer of the film, and the sequence between adsorption of agar(CNT) and PAH(CNT) was reversed, in order to investigate the effect of the adsorption sequence of the film (Fig. 4). It can be seen that the deposition sequence has a marked effect on current density values. When ARS was adsorbed on PAH(CNT), higher current density values were obtained, probably due to electrostatic interactions between the polyelectrolytes. We believe that when ARS was adsorbed on agar, the fact that both have anionic character means that there were repulsive forces

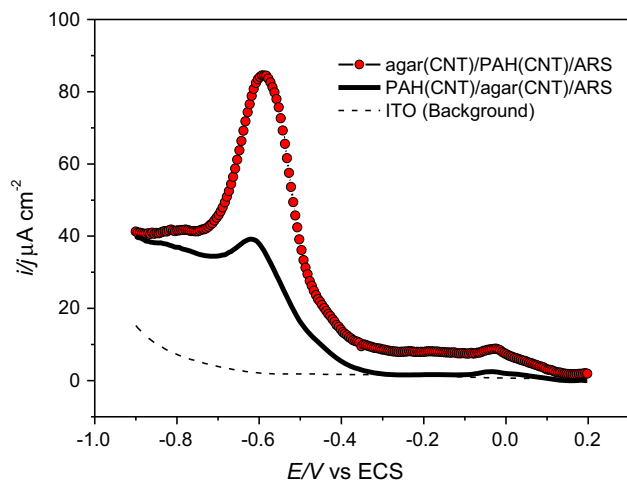


Figure 4 Differential pulse voltammetry comparing the sequence of deposition of trilayer films containing CNTs. All measurements were carried out in 0.1 mol L^{-1} potassium phosphate (pH 7.2), $E_i = -0.9 \text{ V}$, $E_f = 0.2 \text{ V}$, $v = 25 \text{ mV s}^{-1}$.

between these polyelectrolytes, thereby disadvantaging the adsorption of ARS (Fig. 4). It is important to note that regardless of the adsorption architecture, the oxidation process of ARS occurred at -0.5 V , whereas the process of oxidation observed at -0.03 V was maintained in both cases.

Characterization of the films by UV-Vis spectroscopy

UV-Vis spectroscopy allows us to follow the growth of self-assembled films from the increase in the absorbance value in each adsorption step, i.e., at each layer adsorbed [77].

The agar/PAH/ARS and agar(CNT)/PAH(CNT)/ARS films presented two absorption bands, one at 444 nm and the other at 556 nm , attributed, respectively, to the $n\text{-}\delta^*$ transition of the protonated form and deprotonated form of the hydroxyl group on

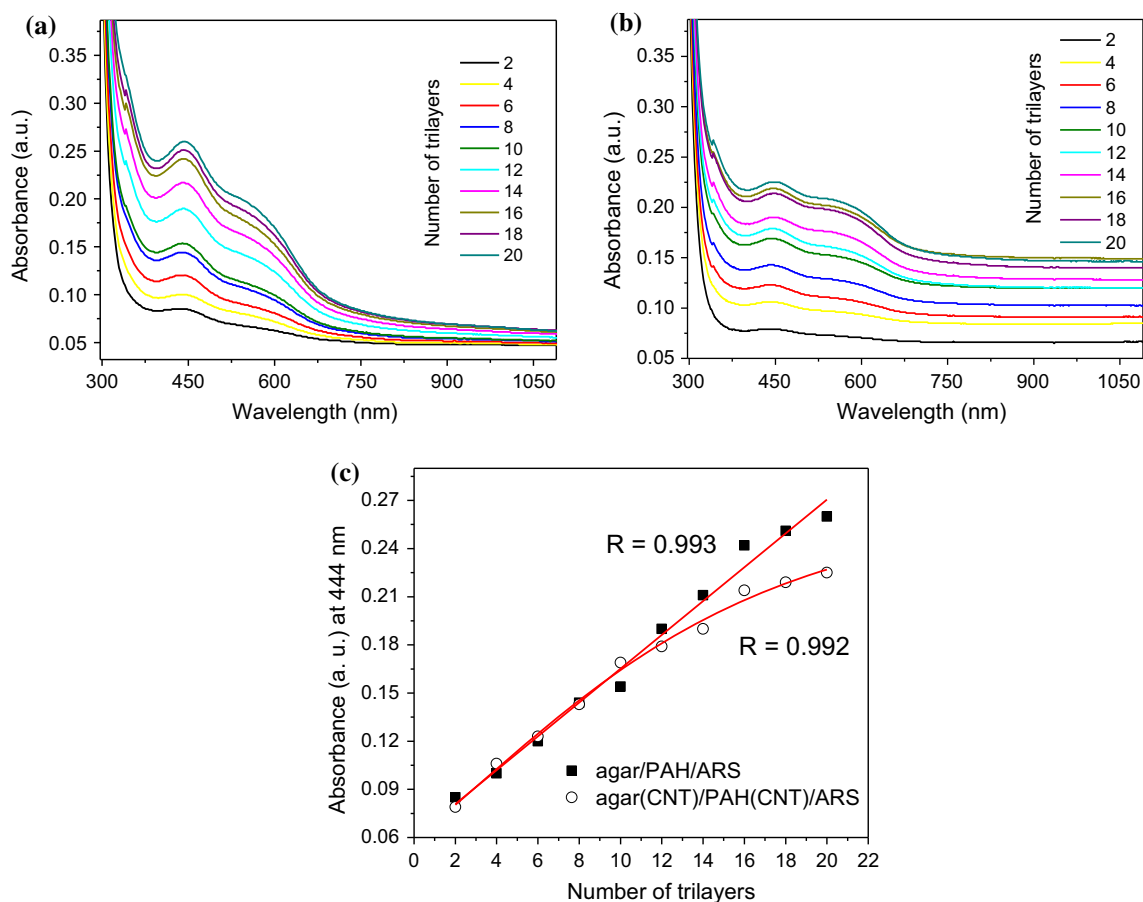
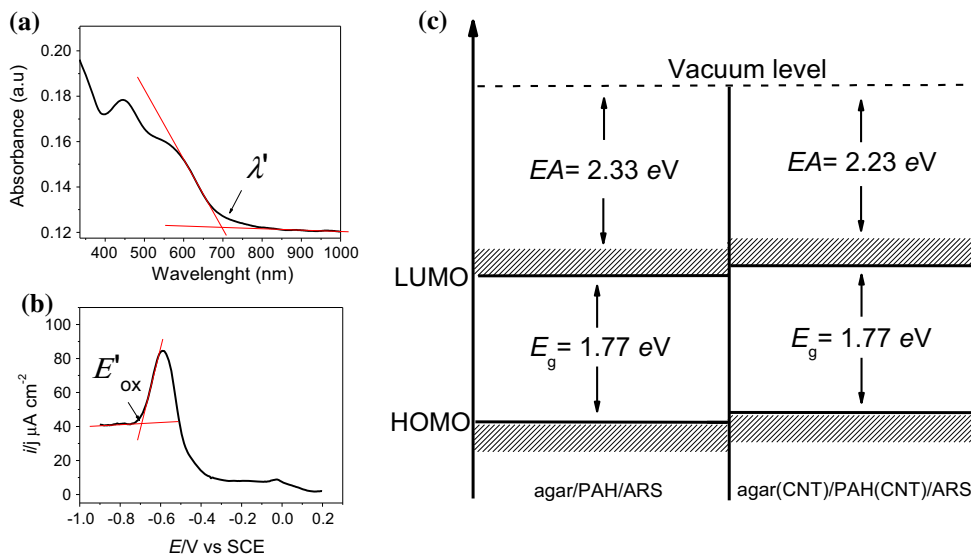


Figure 5 Absorption spectra obtained for every two trilayers adsorbed (n) for the films **a** agar/PAH/ARS and **b** agar(CNT)/PAH(CNT)/ARS. The Inset shows the absorbance obtained for films at 444 nm as function of n .

Figure 6 **a** Obtaining the value of the initial wavelength (λ') and **b** potential of initial oxidation (E'_{ox}). **c** Diagram of the energy levels for the agar/PAH/ARS and agar(CNT)/PAH(CNT)/ARS films.



ARS, the only material present in the film that absorbs in the UV–Vis region [78].

Figure 5 shows the spectra obtained for films of interest in the presence and absence of CNTs. Figure 5a shows the spectra obtained at every two trilayers adsorbed on the agar/PAH/ARS film, while in Fig. 5b the same is shown for the agar(CNT)/PAH(CNT)/ARS system. Figure 5c shows the growth curve of these films, which was constructed from the relationship between the number of trilayers adsorbed and the absorbance for both films at 444 nm.

From Fig. 5c, it can be seen that the nanotubes do not influence considerably the absorbance of the film until the eighth trilayer. Above the eighth trilayer adsorbed, there is a decrease in the absorbance of the film containing the nanotubes, probably due to the increased opacity of the film caused by the presence of the CNTs.

It is noteworthy that the agar/PAH/ARS film showed linear growth, with a correlation coefficient (R) of 0.993, while the agar(CNT)/PAH(CNT)/ARS film presented sigmoidal behavior ($R = 0.992$). This indicates that the thickness of these films can be controlled by the number of adsorbed trilayers through different curve-fitting equations. For the agar/PAH/ARS film, we concluded also that it is a self-regulating system, since it is very close the amounts of material adsorbed by adsorption step [77].

The results obtained by UV–Vis spectroscopy suggest that CNTs play a more important role in

relation to the ARS electroactivity and consecutively of the film than in adsorptive or spectroscopic properties of these films. Accordingly, we believe that the synergy among the CNTs, ARS, and other materials present in the film is responsible for the current increase observed for ARS in Fig. 2, and not simply an increase in the surface area of the film promoted by CNTs.

Construction of the energy diagram

The energy diagrams of LbL films were constructed from the experimental data obtained by both UV–Vis and DPV. The value of the initial wavelength (λ') was obtained from the intersection of the curves of the UV–Vis absorption spectra, Fig. 6a. The potential of the initial oxidation value (E'_{ox}) was obtained from the linear intersection of the growth of the current oxidation and the background of the differential pulse voltammogram (Fig. 6b) [79].

The value of E'_{ox} was substituted in Eq. 1, to obtain the oxidation potential (E_{ox}), considering E_{vac} equals zero, as determined by the literature [80, 81].

$$E_{ox} = E'_{ox} + E_{ESC} \approx E'_{ox} + E_{vac} + 4.7. \quad (1)$$

The value for λ' , Fig. 6a, was used to calculate the energy of the electronic transition (E_g), using Eq. 2, where h is Planck's constant and c is the speed of light.

$$E_g = \frac{hc}{\lambda'} \quad (2)$$

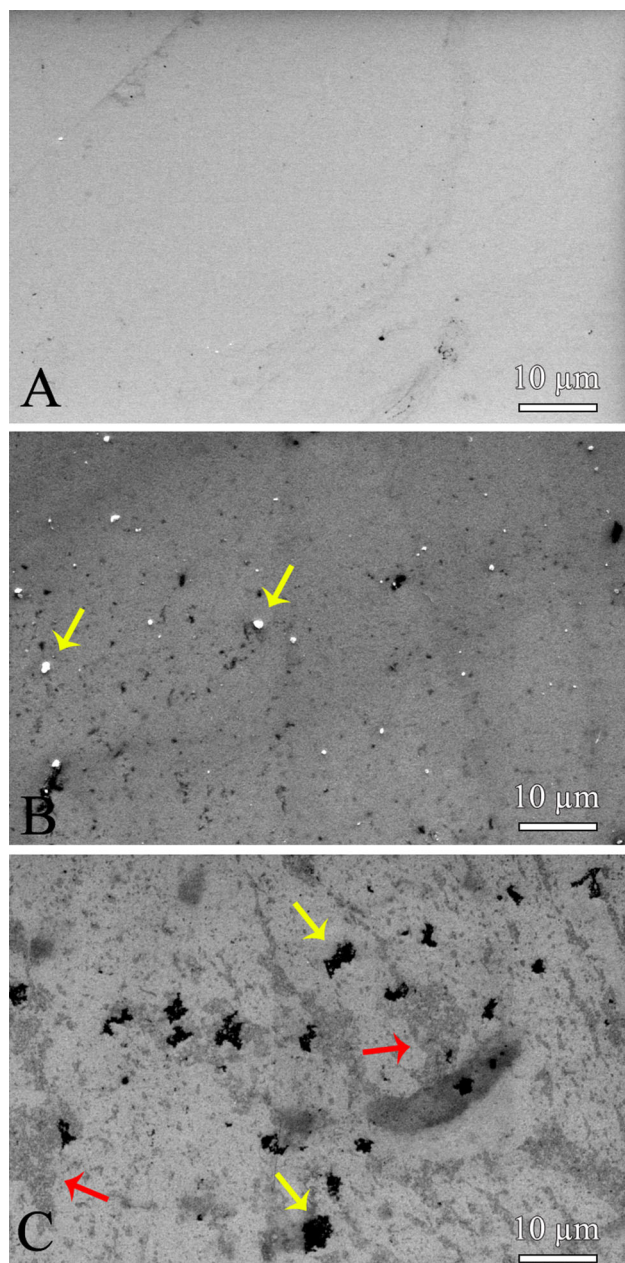


Figure 7 SEM images obtained for **a** ITO and films of **b** agar(CNT)/PAH(CNT)/ARS and **c** agar/PAH/ARS. In **b** yellow arrows indicate the nanotube aggregates. In **c** yellow arrows indicate areas of the substrate that were not covered by the film and the red arrows indicate the distribution of the ARS (medium gray tones).

The ionization potential (IP) was calculated according to Eq. 3, where e is the electron charge.

$$IP = eE_{ox} \quad (3)$$

The electron affinity (EA) was calculated by Eq. 4.

$$EA = IP - E_g \quad (4)$$

Figure 6c shows the energy diagram obtained for the agar/HAP/ARS and agar(CNT)/PAH(CNT)/ARS films. It can be observed that the presence of CNTs improved the conductivity of the film, since they reduced the energy required for the electrons to reach the vacuum level. The electron affinity of ARS with the electrode was increased in the presence of CNTs.

The higher value obtained for the HOMO energy, shown in Fig. 6c, is similar to previously reported results for phthalocyanines [81]. Phthalocyanines are materials used in the construction of optical-electronic devices used in photodynamic therapy, and especially for the development of electrochemical sensors and biosensors. Accordingly, we believe that the films produced here are promising for electronic applications, thus opening prospects for future studies in this area. Moreover, in this study, we also evaluated the potential of the film as a platform for an electrochemical sensor.

SEM morphological analysis

Figure 7 shows the SEM images obtained from the morphological study of the substrate (Fig. 7a) and substrate modified by the LbL films in the presence or absence of carbon nanotubes (CNT), Fig. 7b and c, respectively. It was observed that when the nanotubes were dispersed in the solution of agar and PAH (agar(CNT)/PAH(CNT)/ARS film, Fig. 7b), there was the formation of aggregates with granular form, Fig. 7b. On the other hand, when CNTs were incorporated on the film structure, a more uniform distribution of ARS was promoted, which can be easily observed by comparing Fig. 7b and c. That is, in Fig. 7c the agar/PAH/ARS film (without CNT) showed small areas with medium gray tones, indicating that there is a little amount of ARS distributed on the film, when in the absence of CNTs. These results corroborate with the low current observed for this film in the study shown in Fig. 3. Methods that seek a better dispersion for CNTs can optimize the system proposed here.

Detection tests for hydrogen peroxide

Cyclic voltammetry experiments were carried out in which we examined the response of the agar(CNT)/

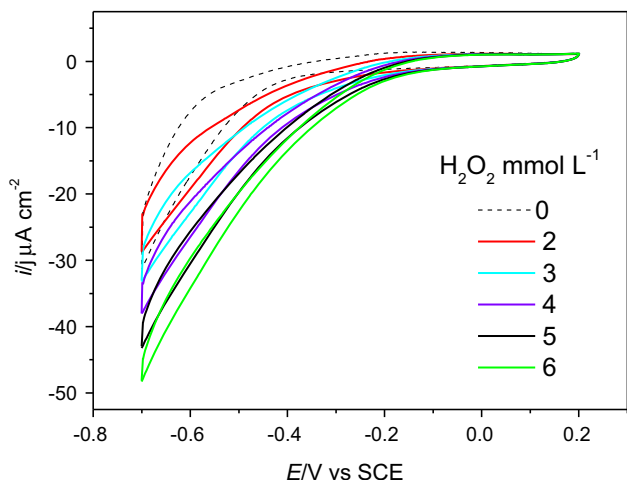


Figure 8 Cyclic voltammograms obtained for the agar(CNT)/PAH(CNT)/ARS film at different concentrations of H₂O₂. The measurements were performed in 0.1 mol L⁻¹ phosphate buffer (pH 7.2), *v* = 50 mV s⁻¹.

PAH(CNT)/ARS in the absence and in the presence of a concentration gradient of H₂O₂ (Fig. 8), to evaluate the potential of the film for reduction of hydrogen peroxide.

It was observed in Fig. 8 that with increasing concentrations of H₂O₂, there was an increase in reduction current from -0.25 V, which increased as the applied potential shifted to more negative values.

Next, the technique of chronoamperometry was used to evaluate the potential of the developed film for the reduction of H₂O₂ under a constant potential. The amperometric measurements were performed to assess the sensitivity, linearity, and time of response of the electrode in the presence of H₂O₂. Various polarization potentials were tested and the most significant results are shown in Fig. 9. The agar(CNT)/PAH(CNT)/ARS film showed better performance when the applied potential was -0.5 V versus SCE, exhibiting a response of less than 5 s, and a stabilizing current of up to 30 s (Fig. 9).

In Fig. 9, it can be observed that, with successive additions of H₂O₂ in the electrochemical cell, there is an increase in the current reduction for hydrogen peroxide, with two distinct regions of linearity. In Fig. 9a, the amperometric response for concentrations from 0.05 to 0.4 mmol L⁻¹ is shown, while in Fig. 9b the amperometric response for concentrations between 3.0 and 8.0 mmol L⁻¹ is shown. The

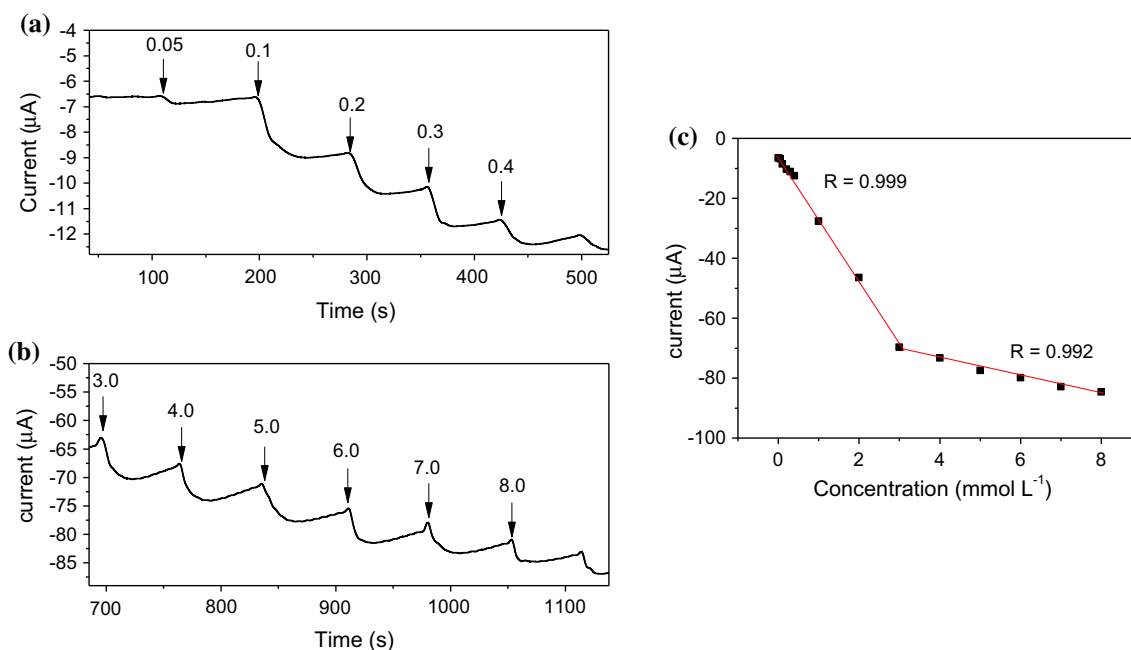


Figure 9 Chronoamperometric response for the agar(CNT)/PAH(CNT)/ARS film in the presence of the H₂O₂ at concentration ranges from **a** 0.05 to 0.4 mmol L⁻¹ and **b** 3.0 to 8.0 mmol L⁻¹. **c** Shows two linear regions between the H₂O₂ concentration and

the average current values registered. All measurements were performed in 0.1 mol L⁻¹ potassium phosphate buffer (pH 7.2). Applied potential = -0.5 V versus SCE.

Table 1 LD found for the H₂O₂ in this study compared to other available in the literature

Non-enzymatic electrochemical sensors for the detection of hydrogen peroxide	Limit of detection/LD (μM)	References
Agar(CNT)/PAH(CNT)/ARS LbL film	0.15	This study
Electrochemical sensor for hydrogen peroxide based on ARS and CNTs	1.2	Han et al. [56]
Vertical NiO nanosheets supported on the graphite sheet	0.4	Liu et al. [82]
Fenton-type reaction on poly(azure A)-chitosan/Cu modified electrode	0.7	Liu et al. [83]
CuO flower-like nanostructured electrode formed by chemical oxidation of copper foil under hydrothermal conditions	0.167	Song et al. [84]
Copper on porous silicon (Cu/PSi) nanocomposite powder synthesized by electrodeless deposition of copper nanoparticles on the etched PSi powder in a solution containing hydrofluoric acid and CuSO ₄	0.27	Ensafi et al. [85]
Non-enzymatic amperometric detection of hydrogen peroxide using grass-like copper oxide nanostructures calcined in nitrogen atmosphere	3.26	Gao et al. [86]
Au electrode modified with polyaniline, multiwalled carbon nanotubes and gold nanoparticles	0.3	Narang et al. [87]
CuS nanoparticles on surface of a glassy carbon electrode (GCE) by drop coating techniques	1.1	Dutta et al. [88]
Nanoporous gold (NPG) fabricated by dealloying Au–Ag film	3.26	Meng et al. [89]
Glassy carbon electrode modified with an MWCNT/polyaniline composite film and platinum nanoparticles	2.0	Zhong et al. [90]
Glassy carbon electrode modified with single-walled carbon nanotubes–manganese complex modified	0.2	Salimi et al. [91]
Graphene wrapped Cu ₂ O nanocubes: non-enzymatic electrochemical sensors for the detection of glucose and hydrogen peroxide with enhanced stability	3.3	Liu et al. [92]

two inclinations obtained in Fig. 9c relate to the two regions of linearity observed, leading us to say that the film is more sensitive to low concentrations of H₂O₂. The detection and quantification limit were estimated at, respectively, 0.15 and 0.21 $\mu\text{mol L}^{-1}$. Table 1 shows the LD found for the H₂O₂ in this study compared to other available in the literature. It is important to mention that the literature already reports an electrochemical sensor for hydrogen peroxide based on ARS and CNTs (Han et al. 2013). However, in this new proposal, substantial improvements in comparison with the sensor published are shown. The LD found in this study was 10 times lower than that reported in the study of Han et al. [56], which in this case was 1.2 mmol L^{-1} . Additionally, the sensor disclosed herein showed linear response at wider concentration range in

comparison with the literature (0.03 a 5.0 mmol L^{-1}).

Additionally, the stability of sensor after successive contacts with the H₂O₂ was evaluated. In these studies, it was observed that the response of agar(CNT)/PAH(CNT)/ARS film in the absence of H₂O₂ was similar to the response of this same film after successive contacts of the electrode with peroxide, i.e., the profile and current density observed in the voltammograms recorded for the films not changed considerably after contact with peroxide, indicating the great potential of this system for the proposed application (see Fig. S3).

The results of this study create a foundation for the implementation of this new material as an electrochemical sensor for H₂O₂. However, new studies should be carried out to evaluate the effect of

interferents in the analytical response of this sensor, as well as validation of the method for its use in peroxide detection in real samples. Also, because it is a new system, different analytes should be tested aiming to expand the applicability of this material, which is currently under study by our group.

Conclusions

For the first time, ARS was immobilized by LbL technique on ITO electrodes. ARS showed electroactivity adsorbed on ITO only when it had been previously modified by agar and PAH. Current values, almost 3 times higher, were obtained when the CNTs were interspersed on the film, thus leading to an improvement in the charge transfer process between ARS and the electrode, probably due to a mechanism of constitutional dynamic chemistry present in the proposed system, and also due to the interactions between the π electrons of ARS and CNTs.

The energy diagrams obtained for the agar/PAH/ARS and agar(CNT)/PAH(CNT)/ARS films showed that the presence of CNTs in the film structure improves the electron affinity between ARS and the ITO electrode. Both films are promising for electronic applications as electrochemical sensors.

The growth curves of the agar/PAH/ARS and agar(CNT)/PAH(CNT)/ARS films obtained by UV-Vis spectroscopy indicated that the nanotubes do not influence significantly the adsorption of ARS up to the eighth trilayer, confirming that the increase in the current observed for ARS was due to the improved transfer of charges promoted by the synergism of the materials present in the film. Morphological analysis performed by SEM showed that although there is the aggregation of CNTs, they promote a more uniform distribution of the ARS in the film.

The agar(CNT)/PAH(CNT)/ARS film exhibited good catalytic response to the reduction of H_2O_2 , reaching a detection limit in the order of $0.21 \mu\text{mol L}^{-1}$.

Acknowledgements

This study received financial support from CNPq and CAPES, Brazil. The authors are grateful to LMMA—Laboratório Multiusuário de Microscopia Avançada, UFPI, Brazil.

Compliance with ethical standards

Conflicts of interest The authors declare that there is no any conflict of interest about this manuscript

Electronic supplementary material: The online version of this article (doi:10.1007/s10853-016-9958-8) contains supplementary material, which is available to authorized users.

References

- [1] Islam N, Miyazaki K (2009) Nanotechnology innovation system: understanding hidden dynamics of nanoscience fusion trajectories. *Technol Forecast Soc Chang* 76:128–140
- [2] Mihindukulasuriya SDF, Lim LT (2014) Nanotechnology-development in food packaging: a review. *Trends Food Sci Technol* 40:149–167
- [3] Romig AD Jr, Baker AB, Johannes J, Zipperian T, Eijkel K, Kirchhoff B, Mani HS, Rao CNR, Walsh S (2007) An introduction to nanotechnology policy: opportunities and constraints for emerging and established economies. *Technol Forecast Soc Change* 74:1634–1642
- [4] Zucolotto V, Ferreira M, Cordeiro MR, Constantino CJL, Moreira WC, Oliveira Jr^o ON (2006) Nanoscale manipulation of polyaniline and phthalocyanines for sensing applications. *Sens Actuators B* 113:809–815
- [5] Brinker CJ, Scherer GW (1990) *Sol-gel science the physical and chemistry of processing*. Academic Press, Boston
- [6] Carvalho CL, Varela JA (2001) Construção e Caracterização de um Equipamento para Deposição de Filmes pela Técnica de Dip-Coating. *Revista de Física Aplicada e Instrumentação* 14:115–119
- [7] Guimarães JA (2009) Estudo de filmes de Langmuir e Langmuir-Blodgett visando o desenvolvimento de biossensor de Colesterol. UFRJ-COPPE, Rio de Janeiro
- [8] Duran N, Matoso LHC, Morais PC (2006) Nanotecnologia: introdução, preparação e caracterização de nanomateriais e exemplos de aplicação. *Artliber* 13–68
- [9] Iler RK (1966) Multilayers of colloidal particles. *J Colloid Interface Sci* 21:569–594
- [10] Decher G (1997) Fuzzy nanoassemblies: toward layered polymeric multicomposites. *Science* 277:1232–1237
- [11] Pereira A, Alves S, Casanova M, Zucolotto V, Bechtold IH (2010) The use of colloidal ferrofluid as building blocks for nanostructured layer-by-layer films fabrication. *J Nanopart Res* 12:2779–2785

- [12] Zucolotto V, Strack PJ, Santos FR, Balogh DT, Constantino CJL, Mendonça CR, Oliveira ON Jr (2004) Molecular engineering strategies to control photo-induced birefringence and surface-relief gratings on layer-by-layer films from an azopolymer. *Thin Solid Films* 453:110–113
- [13] Luz RADS, Martins MVA, Magalhães JL, Siqueira JRS Jr, Zucolotto V, Oliveira ON Jr, Crespilho FN, da Silva WC (2011) Supramolecular architectures in layer-by-layer films of single-walled carbon nanotubes, chitosan and cobalt (II) phthalocyanine. *Mate Chem Phys* 130:12–1077
- [14] Paterno LG, Mattosso LHC, Oliveira Jr^o OND (2000) Filmes Poliméricos Ultrafinos Produzidos pela Técnica de Automontagem: Preparação, propriedades e aplicação. *Quim Nova* 24:228–235
- [15] Huang W, Li X, Xue Y, Huang R, Deng H, Ma Z (2013) Antibacterial multilayer films fabricated by LBL immobilizing lysozyme and HTCC on nanofibrous mats. *Int J Biol Macromol* 53:26–31
- [16] Nakane Y, Kubo I (2009) Layer-by-layer of liposomes and membrane protein as a recognition element of biosensor. *Thin Solid Films* 518:13–681
- [17] Li X, Wang L, Wu Q, Chen Z, Lin X (2014) An enzymatic hydrogen peroxide sensor based on Au–Ag nanotubes and chitosan film. *J Electroanal Chem* 735:13–23
- [18] Ferreira M, Fiorito PA, Torresi SICD (2004) Enzyme-mediated amperometric biosensors prepared with the layer-by-layer (LbL) adsorption technique. *Biosens Bioelectronics* 19:1611–1615
- [19] Zhang SP, Shan LG, Tian ZR, Zheng Y, Shi LY, Zhang DS (2008) Study of enzyme biosensor based on carbon nanotubes modified electrode for detection of pesticides residue. *Chin Chem Lett* 19:592–594
- [20] Souza TTL, Moraes ML, Ferreira M (2013) Use of hemoglobin as alternative to peroxidases in cholesterol amperometric biosensors. *Sens Actuators* 178:13–106
- [21] Wang Y, Hosta-Rigau L, Lomas H, Caruso F (2011) Nanostructured polymer assemblies formed at interfaces: applications from immobilization and encapsulation to stimuli-responsive release. *Phys Chem Chem Phys* 13:4782–4801
- [22] Wuytens P, Parakhonskiy B, Yashchenok A, Winterhalter M, Skirtach A (2014) Pharmacological aspects of release from microcapsules from polymeric multilayers to lipid membranes. *Curr Opin Pharmacol* 18:129–140
- [23] Deng H, Zhou X, Wang X, Zhang C, Ding B, Zhang Q, Du Y (2010) Layer-by-layer structured polysaccharides film-coated cellulose nanofibrous mats for cell culture. *Carbohydr Polym* 80:13–479
- [24] Araújo IMS, Zampa MF, Moura JB, Santos JRDS Jr, Eaton P, Zucolotto V, Veras LMC, de Paula RCM, Feitosa JPA, Leite JRSA, Eiras C (2012) Contribution of the cashew gum (*Anacardium occidentale* L.) for development of layer-by-layer films with potential application in nanobiomedical devices. *Mater Sci Eng* 32:1588–1593
- [25] Barros SBA, Leite CMDS, de Brito ACF, Santos Júnior JRD, Zucolotto V, Eiras C (2012) Multilayer films electrodes consisted of cashew gum and polyaniline assembled by the layer-by-layer technique: electrochemical characterization and its use for dopamine determination. *Int J Anal Chem* 2012:923208
- [26] Ball V (2012) Organic and inorganic dyes in polyelectrolyte multilayer films. *Materials* 05:2681–2704
- [27] Parkes CH (2012) Creating colour in yarn: an introduction to natural dyes. *Ind Crops Prod* 37:408–414
- [28] Shahid M, Ul-Islam S (2013) Recent advancements in natural dye applications: a review. *J Clean Prod* 53:14–331
- [29] Pereira CF, Fernandes EN, Marques EP, Marques AL (2003) Potencialidades Analíticas Do Sistema Cu (II)—Amarelo De Alizarina R: Um novo procedimento espectralítico para determinação de Cu(II) no nível de micromolar e estudos de equilíbrios em solução. *Analytica* 04:53–58
- [30] Gao J, Yu J, Lu Q, He X, Yang W, Pu L, Yang Z (2006) Decoloration of alizarin red S in aqueous solution by glow discharge electrolysis. *Dyes Pigm* 76:47–52
- [31] Cordeiro CRB, Marques ALB, Marques EP, Cardoso WS, Zhang J (2006) Ultra trace copper determination by catalytic-adsorptive stripping voltammetry using an alizarin red S modified graphite electrode. *Int J Electrochem Sci* 1:343–353
- [32] Devi LG, Munikrishnappa C, Nagaraj B, Rajashekhar KE (2013) Effect of chloride and sulfate ions on the advanced photo Fenton and modified photo Fenton degradation process of Alizarin Red S. *J Mol Catal A: Chem* 375:125–131
- [33] Lin X, Ni Y, Kokot S (2013) Glassy carbon electrodes modified with gold nanoparticles for the simultaneous determination of three food antioxidants. *Anal Chim Acta* 765:14–62
- [34] Zhang X, Wei Y, Ding Y (2014) Electrocatalytic oxidation and voltammetric determination of ciprofloxacin employing poly(alizarin red)/graphene composite film in the presence of ascorbic acid, uric acid and dopamine. *Anal Chim Acta* 835:14–36
- [35] Dai HP, Shiu KK (1998) Voltammetric behavior of alizarin red S adsorbed on electrochemically pretreated glassy carbon electrodes. *Electrochim Acta* 43:2709–2715
- [36] Ba X, Luo L, Ding Y, Zhang Z, Chu Y, Wang B, Ouyang X (2012) Poly(alizarin red)/graphene modified glassy carbon electrode for simultaneous determination of purine and pyrimidine. *Anal Chim Acta* 752:14–100
- [37] Gaya UI, Abdullah AH (2008) Heterogeneous photocatalytic degradation of organic contaminants over titanium dioxide: a

- review of fundamentals, progress and problems. *J Photochem Photobiol, C* 9:1–12
- [38] Liu J, Zhou D, Liu X, Wu K, Wan C (2009) Determination of kojic acid based on the interface enhancement effects of carbon nanotube/alizarin red S modified electrode. *Colloids Surf, B* 70:15–24
- [39] Jiang Yuan-Yuan, Kun Wang K, Chong-Zheng Xu, Yang Xiao-Di, Li H (2013) Application of alizarin/graphene-chitosan modified electrode on detection of human telomere DNA. *Chin J Anal Chem* 41:481–487
- [40] de Souza ML, Corio P (2010) Surface-enhanced Raman scattering study of alizarin red S. *Vib Spectrosc* 54(2):137–141
- [41] Roosta M, Ghaedi M, Mohammadi M (2014) Removal of alizarin red S by gold nanoparticles loaded on activated carbon combined with ultrasound device: optimization by experimental design methodology. *Powder Technol* 267:15–144
- [42] Faouzi AM, Nasr B, Abdellatif G (2007) Electrochemical degradation of anthraquinone dye alizarin red S by anodic oxidation on boron-doped diamond. *Dyes Pigment* 73:86–89
- [43] Mouchrek Filho VE, Marques ALB, Zhang JJ, Chierice GO (1999) Complexation of copper(II) with alizarin red S adsorbed on a graphite electrode and its possible application in electroanalysis. *Electroanalysis* 11:1130–1136
- [44] Sousa MFB (1997) Eletrodos quimicamente modificados aplicados à eletroanálise: uma breve abordagem. *Quim Nova* 20:191–195
- [45] Deng H, Zhou X, Wang X, Zhang C, Ding B, Zhang Q, Du Y (2010) Layer-by-layer structured polysaccharides film-coated cellulose nanofibrous mats for cell culture. *Carbohydr Polym* 80:474–479
- [46] Eiras C, Santos AC, Zampa MF, de Brito ACF, Constantino CJL, Zucolotto V, dos Santos JR Jr (2010) Natural polysaccharides as active biomaterials in nanostructured films for sensing. *J Biomater Sci* 21:1533–1543
- [47] He J, Guan Y, Zhang Y (2013) Redox-active LBL films via in situ template polymerization of hydroquinone. *J Appl Polym Sci* 129:3070–3076
- [48] Da Cunha PLR, De Paula RCM, Feitosa JPA (2009) Polissacarídeos da biodiversidade brasileira: uma oportunidade de transformar conhecimento em valor econômico. *Quim Nova* 32:649–660
- [49] Maciel JS, Chaves LS, Souza BWS, Teixeira DIA, Freitas ALP, Feitosa JPA, de Paula RCM (2008) Structural characterization of cold extracted fractions of soluble sulfated polysaccharide from red seaweed *Gracilaria birdiae*. *Carbohydr Polym* 71:559–565
- [50] Jensen A (1993) Present and future needs for algae and algae products. *Hydrobiologia* 260:15–23
- [51] Mchugh D (2003) A guide to the seaweed industry. *FAO Fisheries Tech* 441
- [52] Göpel W, Ziegler CH, Breer H, Schild D, Apfelbach R, Joerges J, Malaka R (1998) Bioelectronic noses: a status report. *Biosens Bioelectron* 13:479–493
- [53] Habibi B, Jahanbakhshi M (2014) A novel nonenzymatic hydrogen peroxide sensor based on the synthesized mesoporous carbon and silver nanoparticles nanohybrid. *Sens Actuators* 203:16–925
- [54] De Mattos IL, Shiraishi KA, Braz AD, Fernandes JR (2003) Peróxido de hidrogênio: importância e determinação. *Quim Nova* 25:373–380
- [55] Chang MCY, Pralle A, Isacoff EY, Chang CJA (2004) Selective, cell-permeable optical probe for hydrogen peroxide in living cells. *J Am Chem Soc* 126:15392–15393
- [56] Han H, Wu X, Wu S, Zhang Q, Lu W, Zhang H, Pan D (2013) Fabrication of alizarin red S/multi-walled carbon nanotube nanocomposites and their application in hydrogen peroxide detection. *J Mater Sci* 48:3422–3427
- [57] Lu X, Zhou J, Lu W, Liu Q, Li J (2008) Carbon nanofiber-based composites for the construction of mediator-free biosensors. *Biosens Bioelectron* 23:1236–1243
- [58] Chen H, Zhang Z, Cai D, Zhang S, Zhang B, Tang J, Wu Z (2011) A hydrogen peroxide sensor based on Ag nanoparticles electrodeposited on natural nano-structure attapulgite modified glassy carbon electrode. *Talanta* 86:16–270
- [59] Li X, Wang L, Wu Q, Chen Z, Lin X (2014) Nonenzymatic hydrogen peroxide sensor based on Au-Ag nanotubes and chitosan film. *J Electroanal Chem* 735:16–23
- [60] Shu X, Chen Y, Yuan H, Gao S, Xiao D (2007) H₂O₂ sensor based on the room-temperature phosphorescence of nano TiO₂/SiO₂ composite. *Anal Chem* 79:3695–3702
- [61] Jia J, Wang B, Wu A, Cheng G, Li Z, Dong S (2002) A method to construct a third-generation horseradish peroxidase biosensor: self-assembling gold nanoparticles to three-dimensional sol-gel network. *Anal Chem* 74:2217–2223
- [62] Wang L, Wang E (2004) A novel hydrogen peroxide sensor based on horseradish peroxidase immobilized on colloidal Au modified ITO electrode. *Electrochem Commun* 6:225–229
- [63] Antuna-Jiménez DM, Blanco-López MC, Miranda-OrdieresAj Lobo-Castanón MJ (2015) Artificial enzyme-based catalytic sensor for the electrochemical detection of 5-hydroxyindole-3-acetic acid tumor marker in urine. *Sens Actuators B Chem* 220:688–694
- [64] Huang S (2008) Detection of *Escherichia coli* using CMOS array photo sensor-based enzyme biochip detection system. *Sens Actuators B* 133:561–564
- [65] Kudo T, Hirano M, Ishihara T, Shimura S, Totani K (2014) Glycopeptide probes for understanding peptide specificity of

- the folding sensor enzyme UGGT. *Bioorg Med Chem Lett* 24:5563–5567
- [66] Liu J, Zhou D, Liu X, Wu K, Wan C (2009) Determination of kojic acid based on the interface enhancement effects of carbon nanotube/alizarin red S modified electrode. *Colloids Surf, B* 70:20–24
- [67] Karuppiaha C, Palanisamy S, Chena S, Veeramani V, Periakaruppanb P (2014) A novel enzymatic glucose biosensor and sensitive non-enzymatic hydrogen peroxide sensor based on graphene and cobalt oxide nanoparticles composite modified glassy carbon electrode. *Sens Actuators B Chem* 196:450–456
- [68] Yagati AK, Lee T, Min J, Choi J (2013) An enzymatic biosensor for hydrogen peroxide based on CeO₂ nanostructure electrodeposited on ITO surface. *Biosens Bioelectron* 47:385–390
- [69] Kern W (1984) Purifying Si and SiO₂ surfaces with hydrogen peroxide. *Semicond Int* 7:94–98
- [70] Mazumber S, Ghosal PK, Pujol CA, Carlucci MJ, Damonte EB, Ray B (2002) Isolation chemical investigation and antiviral activity of polysaccharides from *Gracilariacorticata* (*Gracilariaceae*, *Rhodophyta*). *Int J Biol Macromol* 31:87–95
- [71] Pereira CF, Fernandes EN, Marques EP.; Marques AL (2003) Potencialidades Analíticas Do Sistema Cu (Ii)—Amarelo De Alizarina R: Um novo procedimento espectralítico para determinação de Cu(II) no nível de micromolar e estudos de equilíbrios em solução. *Analytica*, 2003
- [72] Yang L, Zhang L (2009) Chemical structural and chain conformation characterization os some bioactive polysaccharides isolated from natural sources. *Carbohydr Polym* 76:349–361
- [73] Krajewska B (2004) Application of chitin- and chitosan-based materials for enzyme immobilizations: a review. *Enzyme Microb Technol* 35:126–139
- [74] Teixeira PRS, Marreiro ASDN, Farias EADO, Dionisio NA, Silva Filho EC, Eiras C (2015) Layer-by-layer hybrid films of phosphate cellulose and electroactive polymer as chromium (VI) sensors. *J Solid State Electrochem* 19: 2129–2139
- [75] Farias EAO, dos Santos MC, Dionisio NA, Quelemes PV, Leite JRS, Eaton P, da Silva DA, Eiras C (2015) Layer-by-layer films based on biopolymers extracted from red seaweeds and polyaniline for applications in electrochemical sensors of chromium VI. *Mater Sci Eng, B* 200:9–21
- [76] Zhang J, Li X, Jing Tian LuY, Shi X, Zhan Y, Du Y, Liu H, Deng H (2015) Antimicrobial activity and cytotoxicity of nanofibrous mats immobilized with polysaccharides-rectorite based nanogels. *Colloids Surf, B* 133:370–377
- [77] Thomas O, Burgess C (2007) UV–visible spectroscopy of water and wastewater. Elsevier, The Netherlands
- [78] Grucela-ZajacM Filape M, Skorka L, Bijak K, Smolarek K, Mackowski S, Schab-Balcerzal E (2014) Photophysical, electrochemical and thermal properties of new (co)polyimides incorporating oxadiazole moieties. *Synth Met* 188:161–174
- [79] Micaroni LM, Nart FN, Hümmelgen IH (2002) Considerations about the electrochemical estimation of the ionization potential of conducting polymers. *J Solid State Electrochem* 7:55–59
- [80] Crespilho FN, Zucolotto V, Siqueira JR, Carvalho AFJ, Nart FC, Oliveira ON (2006) Using electrochemical data to obtain energy diagrams for layer-by-layer films from metallic phthalocyanines. *Int J Electrochem Sci* 1:151–159
- [81] Zampa MF, Brito ACF, Kitagawa IL, Constantino CJL, Oliveira ON Jr, Cunha HN, Zucolotto V, Santos JRC Jr (2007) Natural Gum assisted phthalocyanine immobilization in electroactive nanocomposite physicochemical characterization and sensing applications. *Biomacromolecules* 8:3408–3413
- [82] Liu W, Zhang H, Yang B, Li Z, Lie L, Zhang X (2015) A non-enzymatic hydrogen peroxide sensor based on vertical NiO nanosheets supported on the graphite sheet. *J Electroanal Chem* 749:62–67
- [83] Liu T, Luo Y, Wang W, Kong L, Zhu J, Tan L (2015) Non-enzymatic detection of hydrogen peroxide based on Fenton-type reaction on poly(azure A)-chitosan/Cu modified electrode. *Electrochim Acta* 182:742–750
- [84] Song MJ, Hwang SW, Whang D (2010) Non-enzymatic electrochemical CuO nanoflowers sensor for hydrogenperoxide detection. *Talanta* 80:1648–1652
- [85] Ensafi AA, Abarghoui MM, Rezaei B (2014) Electrochemical determination of hydrogen peroxide using copper/porous silicon based non-enzymatic sensor. *Sens Actuators B Chem* 196:398–405
- [86] Peng Gao P, Gong Y, Mellott NP, Liu D (2014) Non-enzymatic amperometric detection of hydrogen peroxide using grass-like copper oxide nanostructures calcined in nitrogen atmosphere. *Sens Actuators B Chem* 196:398–405
- [87] Narang J, Nidhi Chauhan N, Pundir CS (2011) A non-enzymatic sensor for hydrogen peroxide based on polyaniline, multiwalled carbon nanotubes and gold nanoparticles modified Au electrode. *Analyst* 136:4460–4466
- [88] Dutta AK, Sudipto Das S, Samanta PK, Roy S, Adhikary B, Biswas P (2014) Non-enzymatic amperometric sensing of hydrogen peroxide at a CuS modified electrode for the determination of urine H₂O₂. *Electrochimica Acta* 144:282–287
- [89] Meng F, Yan X, Liu J, Gu J, Zou Z (2011) Nanoporous gold as non-enzymatic sensor for hydrogen peroxide. *Electrochim Acta* 56:4657–4662

- [90] Zhong H, Yuan R, Chai Y, Zhang Y, Wang C, Jia F (2012) Non-enzymatic hydrogen peroxide amperometric sensor based on a glassy carbon electrode modified with an MWCNT/polyaniline composite film and platinum nanoparticles. *Microchim Acta* 176:389–395
- [91] Salimi A, Mahdioun M, Noorbakhsh A, Abdolmaleki A, Ghavami R (2011) A novel non-enzymatic hydrogen peroxide sensor based on single walled carbon nanotubes–manganese complex modified glassy carbon electrode. *Electrochim Acta* 56:3387–3394
- [92] Liu M, Liu R, Chen W (2013) Graphene wrapped Cu₂O nanocubes: non-enzymatic electrochemical sensors for the detection of glucose and hydrogen peroxide with enhanced stability. *Biosens Bioelectron* 45:206–212